


Article

Ecosystem-Dependent Responses of Vegetation Coverage on the Tibetan Plateau to Climate Factors and Their Lag Periods

Shuohao Cai, Xiaoning Song *, Ronghai Hu  and Da Guo

College of Resources and Environment, University of the Chinese Academy of Sciences, Beijing 100049, China; caishuohao19@mailsucas.ac.cn (S.C.); huronghai@ucas.ac.cn (R.H.); guoda18@mailsucas.ac.cn (D.G.)

* Correspondence: songxn@ucas.ac.cn

Abstract: The spatiotemporal variation characteristics of the Normalized Difference Vegetation Index (NDVI) and its climate response patterns are of significance in deepening our understanding of regional vegetation and climate change. The response of vegetation to climate factors varies spatially and may have lag periods. In this paper, we studied the spatiotemporal responses of vegetation to climatic factors on an ecosystem-dependent scale using GIMMS NDVI3g data and climatic parameters. Pure pixels with a single vegetation type were firstly extracted to reduce the influence of mixed vegetation types. Then, a lag correlation analysis was used to explore the lag effects of climatic parameters affecting NDVI. Finally, the stepwise regression method was adopted to calculate the regression equation for NDVI and meteorological data with the consideration of effect lag times. The results show that precipitation has significant lag effects on vegetation. Temperature is the main climatic factor that affects most vegetation types at the start of growing season. At the end of growing season, the temperate desert, temperate steppe, and temperate desert steppe are greatly affected by precipitation. Moreover, the alpine steppe, alpine desert, alpine meadow, and alpine sparse vegetation are greatly affected by temperature. The needleleaf forest, subalpine scrub, and broadleaf evergreen forest are sensitive to sunshine percentage during almost the whole growing season. These findings could contribute to a better understanding of the drivers and mechanisms of vegetation degradation on the Tibetan Plateau.

Keywords: NDVI; ecosystem-dependent scale; lag effect; climate factors; the Tibetan Plateau



Citation: Cai, S.; Song, X.; Hu, R.; Guo, D. Ecosystem-Dependent Responses of Vegetation Coverage on the Tibetan Plateau to Climate Factors and Their Lag Periods. *ISPRS Int. J. Geo-Inf.* **2021**, *10*, 394. <https://doi.org/10.3390/ijgi10060394>

Academic Editor: Wolfgang Kainz

Received: 15 April 2021

Accepted: 4 June 2021

Published: 7 June 2021

Publisher's Note: MDPI stays neutral with regard to jurisdictional claims in published maps and institutional affiliations.



Copyright: © 2021 by the authors. Licensee MDPI, Basel, Switzerland. This article is an open access article distributed under the terms and conditions of the Creative Commons Attribution (CC BY) license (<https://creativecommons.org/licenses/by/4.0/>).

1. Introduction

The ecosystems on the Tibetan Plateau are very fragile, and their ability to resist disturbance and regenerate is weak [1]. The temperature of the Tibetan Plateau has been constantly increasing due to global warming, and the rate of warming on the Plateau is higher than in other parts of China [1,2]. The study of the spatial and temporal distribution characteristics of vegetation, and its climate response, on the Tibetan Plateau is significant for deepening the understanding of trends in the ecological effects of climate change on vegetation degradation.

The impact of climate change on vegetation occurs at different spatial and temporal scales, and it is difficult to meet the requirements for monitoring changes at regional or global scales with traditional monitoring methods [3]. With its rapid development, remote sensing technology has realized the long-term monitoring of the dynamic changes in vegetation cover in certain regions, which has improved data availability for research on vegetation responses to climate [4]. Based on the fact that chlorophyll absorbs red light, whereas the mesophyll leaf structure scatters near-infrared light [5,6], the Normalized Difference Vegetation Index (NDVI) is derived from the red and near-infrared reflectance captured by the sensor of the satellite: $NDVI = (NIR - RED) / (NIR + RED)$, where NIR and RED are the red and near-infrared light reflected by vegetation. This index can reflect the green plant biomass and green leaf area [5], which has a reliable correlation with

vegetation productivity and is related to the fraction of absorbed photosynthetic radiation intercepted (fAPAR) [7]. NDVI from the Moderate-Resolution Imaging Spectroradiometer (MODIS) and Advanced Very High-Resolution Radiometer (AVHRR) are widely used for the successful assessment, detection, and depiction of landscape conditions and their responses to climate variations at both global and regional scales [8].

Although NDVI data are strongly related to climatic parameters, these relationships are ecosystem-dependent, highly site-specific [9,10] and vary widely in different ecosystems, such as soil [11] and vegetation ecosystems [12]. At present, most studies have examined the relationship between climate and vegetation at different scales. Due to stratified heterogeneity, considering the property information (i.e., vegetation type, land cover type, etc.) of each pixel is very useful for understanding the mechanisms of the effect of climate on vegetation. Therefore, it is important to study the relationship between vegetation and climate factors at sub-regional scales. Among the many potential spatial scales for studies, it is the most reasonable to explore climatic effects on different vegetation ecosystems (i.e., at the vegetation type scale). The response of different grassland systems to climate change can vary greatly [13]. The same type of vegetation will often have a similar climatic environment and similar response mechanisms to climatic factors [14,15].

For a long time, temperature and water stress have been the primary considerations in studies looking at the climate factors affecting vegetation [16]. As research progresses, an increasing number of climate factors are being considered. Sunlight, i.e., solar radiation, provides an energy source for vegetative photosynthesis. On the Tibetan Plateau, sunshine has a more significant impact on vegetation in the south-east region of the Plateau [16]. The lack of radiation observation sites may be the main reason why the influence of radiation is rarely considered in studies, but the sunshine percentage may be a feasible replacement. The relative humidity can reflect the dry and wet conditions of an area to some extent, and can have interactive effects with vegetation [17]. Minimum temperature resistance can be a significant influencing factor on vegetation [18,19].

The effect of precipitation on vegetation shows significant lag [3]. Many studies have been carried out on the effects of lagged precipitation on vegetation growth, indicating that the lag time of the climate factors that affect vegetation growth varies among different vegetation ecosystems and growth stages [4,19–22]. In addition to precipitation, some studies have been conducted on the lag effects of other climate factors on vegetation. Piao (2003) analyzed the monthly average NDVI variation and found that NDVI in April or May was significantly correlated with the temperature in February [23]. Wen et al. (2017) analyzed the regional differences in the lag time of effects at the pixel scale, concluding that there was regional heterogeneity in the amount of lag in the effects of both precipitation and temperature [24]. Revealing the lag in the effects of climate factors on vegetation is significant for understanding the ecological mechanisms of vegetation change.

In this study, long-term GIMMS (Global Inventory Modelling and Mapping Studies) NDVI data, as well as the precipitation, average temperature, average minimum temperature, average maximum temperature, relative humidity and sunshine percentage of the month were collected to study the spatiotemporal variation patterns of vegetation on the Tibetan Plateau, and the ecological responses of vegetation to climatic factors from 1985 to 2015. Based on the 1:1,000,000 vegetation type data for China, ten vegetation domain types and pure pixels for each type of vegetation were selected as the study area to reduce errors due to the coarse spatial resolution of the NDVI dataset used here. To clarify the ecological responses of these vegetation types to climate factors, attribution analysis was performed with the consideration of lag effects. This article is organized as follows: Section 2 gives a brief introduction of the study area, datasets and methods; Section 3 is the presentation of the results; a further discussion is shown in Section 4, and the conclusion is given in Section 5.

2. Materials and Methods

2.1. Study Area

The Tibetan Plateau (Figure 1) lies in the northwest of China, extending from the southern edge of the Himalayas to the northern edge of the Kunlun, Altun and Qilian Mountains ($26^{\circ}00' \sim 39^{\circ}47' \text{ N}$, $73^{\circ}19' \sim 104^{\circ}47' \text{ E}$). Its western border is formed by the Pamir Plateau and Karakorum Mountains, and its eastern and northeastern areas are connected with the western Qinling Mountains and the Loess Plateau. The Tibetan Plateau has a large altitudinal variation from 92 to 7370 m. The climate of the Tibetan Plateau is generally characterized by strong radiation, high sunshine, low overall temperature, large diurnal temperature differences, distinct dry and wet seasons, a warm and wet climate in the southeast and a dry and cold climate in the northwest, as well as a decreasing trend of precipitation and temperature from the southeast to the northwest.

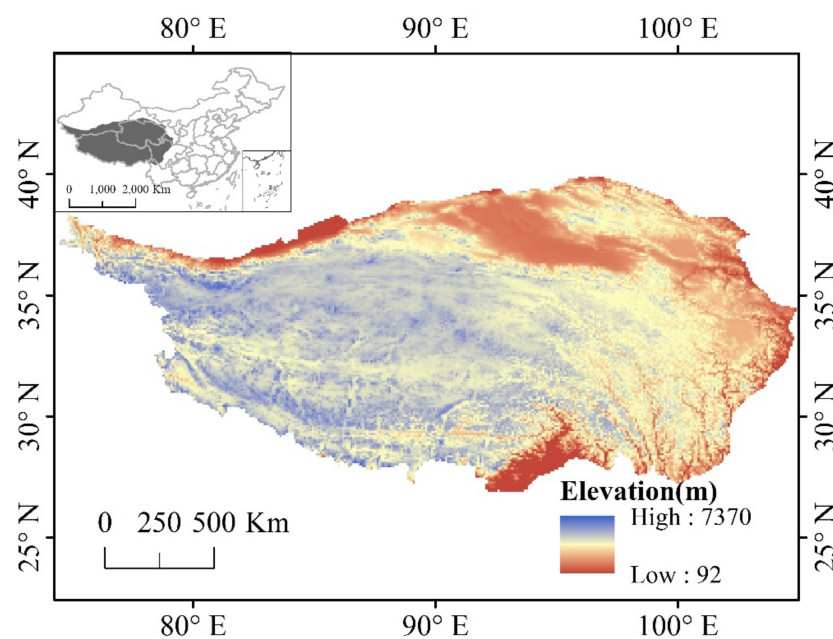


Figure 1. The location and elevation of the study area. The digital elevation data were downloaded from the Resource and Environment Data Cloud Platform (<http://www.resdc.cn/> accessed on 14 April 2021).

2.2. Data Collection

2.2.1. NDVI Data

Because the NDVI is directly correlated with vegetation productivity, there are many possible applications of the NDVI for ecological purposes [7]. NDVI data from the AVHRR dataset have the advantages of a long-time sequence, wide coverage and high accuracy, which is currently considered as one of the best datasets for long-term NDVI analysis.

The GIMMS3g NDVI has been made publicly available on the Internet (<http://www.noaa.gov> accessed on 14 April 2021). We obtained the third-generation dataset recently released by the GIMMS of the National Aeronautics and Space Administration (NASA) from the Internet with a data range from 1985 to 2015, with a spatial resolution of $8 \times 8 \text{ km}$ and a temporal resolution of 16 days. We converted the original HDF format data to TIFF format data in MATLAB. To obtain the monthly NDVI data, the 16-day resolution data were synthesized using the maximum value composites (MVC) method in MATLAB, which can minimize the influence of clouds and the direction of reflection, reduce the effects of the sun angle and shadow, and minimize the effects of aerosols and water vapor [25].

2.2.2. Climate Data

Meteorological data were collected from 176 meteorological stations in the administrative region of the Tibetan Plateau. We obtained monthly ground climate data for China from 1985 to 2015 from the China Meteorological Data Service Centre (CMDSC). In this study, six meteorological factors, namely, average precipitation, average temperature, average maximum temperature, average minimum temperature, monthly sunshine percentage and average relative humidity were considered, and these meteorological data were interpolated into raster data with the same spatial resolution as the NDVI data for further correlation analysis.

Kriging and AUNSPLINE interpolation methods were used to interpolate the meteorological data. By introducing elevation as a covariable, the interpolation accuracy of elevation-related meteorological parameters can be improved significantly using AUNSPLINE. To test the accuracy of the results of the two methods, we used a cross-validation method to test the interpolation results and mainly investigated three parameters: mean absolute error (MAE), mean relative error (MRE), and root mean square error (RMSE).

In the validation method, points were selected three times (groups 1, 2 and 3 in Figure 2) for cross-validation. Fifteen sample points were randomly selected each time from 176 samples as verification points, and the other points were used for interpolation. The interpolation results for 15 sample points were extracted as predicted values, and relevant data for 45 verification points were ultimately obtained. The accuracy of the two interpolation results was compared by calculating the three error parameters between the predicted value and the actual value of the 45 verification points. Meteorological data from June 1995 were used as the validation data. The analysis of the error results showed that the accuracy of AUNSPLINE is higher than that of the kriging method for the temperature interpolation (shown as Table 1). In this paper, the AUNSPLINE interpolation method was used for the average temperature, average minimum temperature, and average maximum temperature, and the kriging interpolation method was used for precipitation, sunshine percentage, and relative humidity.

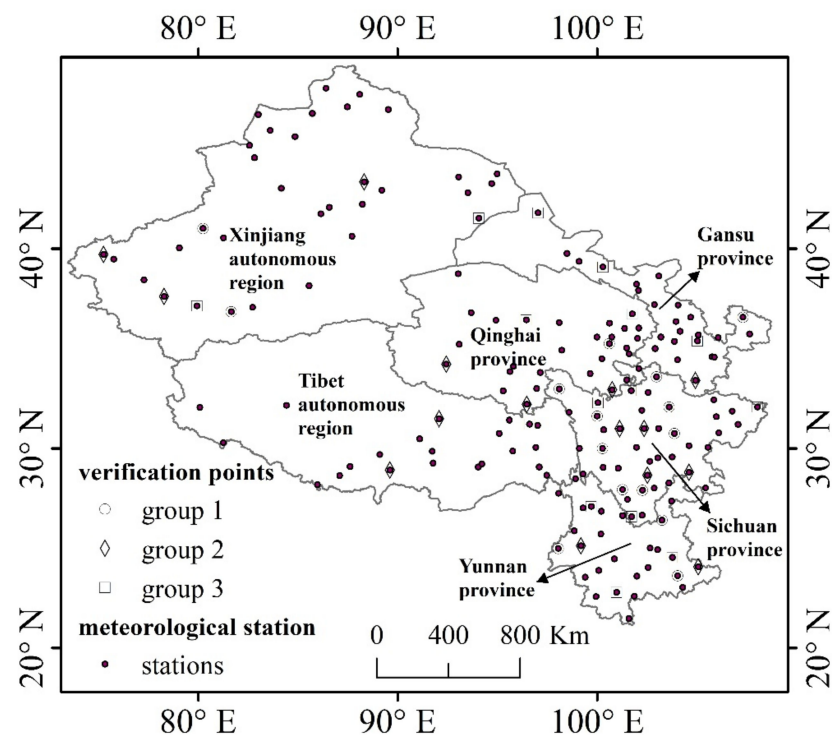


Figure 2. The distribution of meteorological stations and the selection of verification points (groups 1–3).

Table 1. Comparison of the interpolation results from the kriging and AUNSPLINE methods.

Parameters	MAE		MRE		RMSE	
	Kriging	AUNSPLINE	Kriging	AUNSPLINE	Kriging	AUNSPLINE
Average temperature (°C)	1.7495	1.2408	0.099	0.0706	2.3381	1.7488
Average minimum temperature (°C)	1.5332	1.4327	0.1771	0.1655	2.4575	1.9991
Average maximum temperature (°C)	2.4547	1.6747	0.0847	0.0578	3.2046	2.3257
Sunshine percentage (%)	3.4083	4.1973	0.0721	0.0888	4.4182	5.2567
Relative humidity (%)	2.9504	4.9389	0.047	0.0787	4.5443	6.3366
Precipitation (mm)	23.3299	28.646	0.2275	0.2793	35.2529	40.0954

MAE: mean absolute error; MRE: mean relative error; RMSE: root mean square error.

2.2.3. Vegetation Type

The vegetation type data used were the 1:100,000 spatial distribution data on vegetation types in China (grid data with 1-kilometre spatial resolution), which were provided by the Resource and Environment Data Cloud Platform (<http://www.resdc.cn/> accessed on 14 April 2021). This dataset reflects the actual distribution of more than 2000 dominant plant species, as well as the major crops and cash crops in China, and is the authoritative dataset for vegetation type coverage in China.

2.3. Methods

First, based on the vegetation type data with a higher spatial resolution, we obtained (as far as possible) pure pixels of NDVI data, in which homogeneous vegetation exists. Then, we divided the research area into ecosystem-dependent sub-regions. We tested the variation trend in the NDVI time-series data with Mann–Kendall and Sen’s slope method. These two methods are nonparametric methods that require only that the data be independent, regardless of whether the data are normally distributed [26]. Then, the lag correlation coefficient method was used to calculate the lag time of the vegetation response to the climate factors. Finally, stepwise regression was used to determine the factors influencing vegetation change.

2.3.1. Ecosystem-Dependent Sub-Regions

The vegetation type data are the basis of the regional classification in this study. The study area was divided into sub-regions according to the 1:100,000 vegetation dataset of China. GIMMS NDVI3g data have a coarse resolution of approximately 8 km. To a large extent, NDVI pixels are mixed and include a variety of land types or vegetation types. Therefore, we selected pure pixels as the study area to reduce the errors resulting from mixed pixels that contain a variety of ground object information. To select these pure pixels, NDVI data and vegetation raster data with higher resolution were raster-overlaid, and only those pixels with homogeneous vegetation (the number of pixels of this vegetation type accounts for more than 80% of the total vegetation pixels within a pixel of NDVI data) were considered as the study area. In this way, we selected 10 dominant vegetation types on the Tibetan Plateau (Figure 3 and Table 2), and any other vegetation occupying smaller areas was ignored. There are dense climate stations in most areas of Tibetan Plateau (Figure 3). The alpine steppe, alpine desert, temperate desert steppe, and temperate desert distributed in the western region of the Tibetan Plateau are overlaid with sparse meteorological stations.

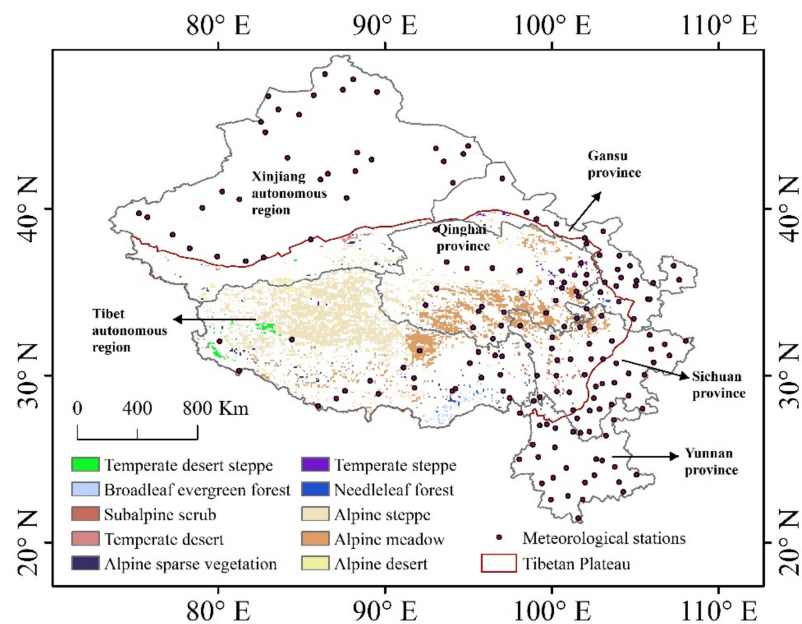


Figure 3. The spatial distribution of ten dominant vegetation types of Tibetan Plateau overlapped with meteorological stations.

Table 2. Ten dominant vegetation types with pure pixels, their ecosystems, and the number of pixels.

Parameters	Subcategory	Number of Pixels
Alpine Steppe	Alpine Grass, Carex Steppe	3479
Alpine Meadow	Alpine Kobresia spp., Forb Meadow	2401
Alpine Desert	Alpine Tussock Dwarf Semishrubby Desert	177
Temperate Desert Steppe	Temperate Dwarf Needlegrass, Dwarf Semishrubby Desert Steppe	112
Alpine sparse vegetation	Alpine sparse vegetation	111
Subalpine Scrub	Subalpine Broadleaf Evergreen Sclerophyllous Scrub	94
Needleleaf Forest	Subtropical and Tropical Mountains Needleleaf Forest	90
Broadleaf Evergreen Forest	Subtropical Monsoon Broadleaf Evergreen forest	73
Temperate Desert	Temperate semishrubby and dwarf semishrubby desert	73
Temperate Steppe	Temperate Needlegrass Arid Steppe	63

Due to the difference in the ecosystem distribution over the Tibetan Plateau, the number of selected pure pixels varies significantly in each vegetation type. The number of pure pixels in the alpine steppe is 3479, while that of the temperate steppe is 63 (Table 2). We randomly selected 50, 500, 1000, 2000 pixels from the total pixels (whole region) as four sub-regions in the alpine steppe, respectively, to explore the effects of imbalance of input data. Then, the Pearson correlation coefficients between the regional average variables of the five regions (four sub-regions and the whole region) in June were obtained (Table 3). The results show that no significant difference exists in different numbers of pixels. Concerning regional average value, the imbalance of the input data has slight effects on the statistical results. Therefore, we used the selected pure pixels in Table 2 as input data for further statistical analysis.

Table 3. Pearson correlation coefficients between the regional average variables of the five regions (four sub-regions and the whole region) in June during the study period.

Variables	Regions	Sub-Region 1	Sub-Region 2	Sub-Region 3	Sub-Region 4	Whole Region
NDVI	Sub-region 1	1.000				
	Sub-region 2	0.977	1.000			
	Sub-region 3	0.980	0.998	1.000		
	Sub-region 4	0.981	0.997	0.999	1.000	
	Whole region	0.980	0.998	0.999	1.000	1.000
Average temperature	Sub-region 1	1.000				
	Sub-region 2	0.468	1.000			
	Sub-region 3	0.368	0.889	1.000		
	Sub-region 4	0.456	0.944	0.959	1.000	
	Whole region	0.440	0.940	0.970	0.990	1.000
Average maximum temperature	Sub-region 1	1.000				
	Sub-region 2	0.987	1.000			
	Sub-region 3	0.985	0.999	1.000		
	Sub-region 4	0.986	0.998	0.999	1.000	
	Whole region	0.986	0.999	0.999	1.000	1.000
Average minimum temperature	Sub-region 1	1.000				
	Sub-region 2	0.977	1.000			
	Sub-region 3	0.975	0.997	1.000		
	Sub-region 4	0.974	0.997	0.999	1.000	
	Whole region	0.976	0.998	0.999	1.000	1.000
Sunshine percentage	Sub-region 1	1.000				
	Sub-region 2	0.991	1.000			
	Sub-region 3	0.990	0.999	1.000		
	Sub-region 4	0.990	0.999	1.000		
	Whole region	0.991	0.999	1.000	1.000	
Relative humidity	Sub-region 1	1.000				
	Sub-region 2	0.989	1.000			
	Sub-region 3	0.989	0.998	1.000		
	Sub-region 4	0.989	0.998	1.000	1.000	
	Whole region	0.989	0.998	1.000	1.000	1.000
precipitation	Sub-region 1	1.000				
	Sub-region 2	0.982	1.000			
	Sub-region 3	0.981	0.997	1.000		
	Sub-region 4	0.982	0.998	0.999	1.000	
	Whole region	0.983	0.998	0.999	1.000	1.000

Sub-region 1: random 50 pixels from total pixels; sub-region 2: random 500 pixels from total pixels; sub-region 3: random 1000 pixels from total pixels; sub-region 4: random 2000 pixels from total pixels; whole region: total pixels.

2.3.2. Sen's Slope and Mann–Kendall Method

To determine the change trends in the time-series NDVI, a Theil–Sen median trend analysis was adopted. The method is a robust nonparametric statistical method, and the formula is:

$$\beta = \text{median}\left(\frac{\text{NDVI}_j - \text{NDVI}_i}{j - i}\right) \quad (1)$$

where NDVI_i and NDVI_j are the NDVI in years i and j ($1985 \leq i, j \leq 2015$). When $\beta < 0$, it indicates that the NDVI increased during this period. When $\beta > 0$, it indicates that the NDVI decreased during this period.

The Mann–Kendall test is a relatively common time-series trend test method that has been widely used in meteorology and hydrology [27]. It is a nonparametric test method. The test formulas are listed below:

$$Q = \sum_{j=1}^{n-1} \sum_{i=j+1}^n \text{sign}(x_i - x_j) \quad (2)$$

$$\text{sign}(x) = \begin{cases} 1, & s > 0 \\ 0, & s = 0 \\ -1, & s < 0 \end{cases} \quad (3)$$

$$Z = \begin{cases} \frac{Q-1}{\sqrt{\text{var}(Q)}}, & Q > 0 \\ 0, & Q = 0 \\ \frac{Q-1}{\sqrt{\text{var}(Q)}}, & Q < 0 \end{cases} \quad (4)$$

where Q is the test statistic, Z is the standardized test statistic, x_i and x_j are time-series data; n is the number of samples. When $n \geq 8$, the result Q approximately follows a normal distribution. Its mean and variance are computed using Equations (5) and (6).

$$E(Q) = 0 \quad (5)$$

$$\text{var}(Q) = \frac{n(n-1)(n-2)}{18} \quad (6)$$

2.3.3. Lag Correlation Coefficient

Based on the understanding that the impact of climate change on vegetation occurs with a certain time lag, we adopted the lag correlation coefficient method to determine the lag period for the impact of climate factors on vegetation. Using this method, we calculated the correlation coefficient between the NDVI and each climate factor in the current month, as well as each climate factor in the previous 1–3 months. When the correlation coefficient reaches the maximum, the correlation between the vegetation NDVI and the climate factor is the strongest, which means that the vegetation had the strongest response to the climate factor in that month, and the lag time was recorded. The lag correlation coefficient is computed using Equation (7).

$$R_m = \max(R_0, R_1, R_2, \dots, R_n) \quad (7)$$

where R_m is the lag correlation coefficient; R_1, R_2, \dots , and R_n are the current month, the month before the current month, the month two months before the current month, \dots , and the month n months before the current month, respectively; m is the lag time.

2.3.4. Stepwise Regression

Stepwise regression is a method of fitting regression models where variables are considered one at a time for addition to or subtraction from a set of independent variables based on some criteria. This regression method can eliminate strong correlations between variables to some extent and exclude variables that are not statistically significant [28]. Here, NDVI is the dependent variable, and the precipitation, average temperature, average minimum temperature, average maximum temperature, relative humidity, sunshine percentage are independent variables. The independent variables are first standardized. Whether the independent variable is added to the equation is determined by a sequence of F-tests. The stepwise regression used here performs a forward-backward feature selection based on the significant test (p -value). And in each step, this model will include a feature if its p -value less than 0.01 and exclude a feature if its p -value greater than 0.05. Ultimately, the corresponding variable was added to the regression equation.

3. Results

3.1. The Variation Trends and Spatial Distribution Characteristics of NDVI on the Tibetan Plateau

The annual variation in the monthly average NDVI of most vegetation types on the Tibetan Plateau showed the same change trend, with only a single peak characteristic across the 31 years (Figure 4). In most vegetation types, NDVI begins to rise from April and reaches a maximum value in the period between August and September, which is the

stage of vegetation growth. Therefore, April to September was used as the analysis period in this study.

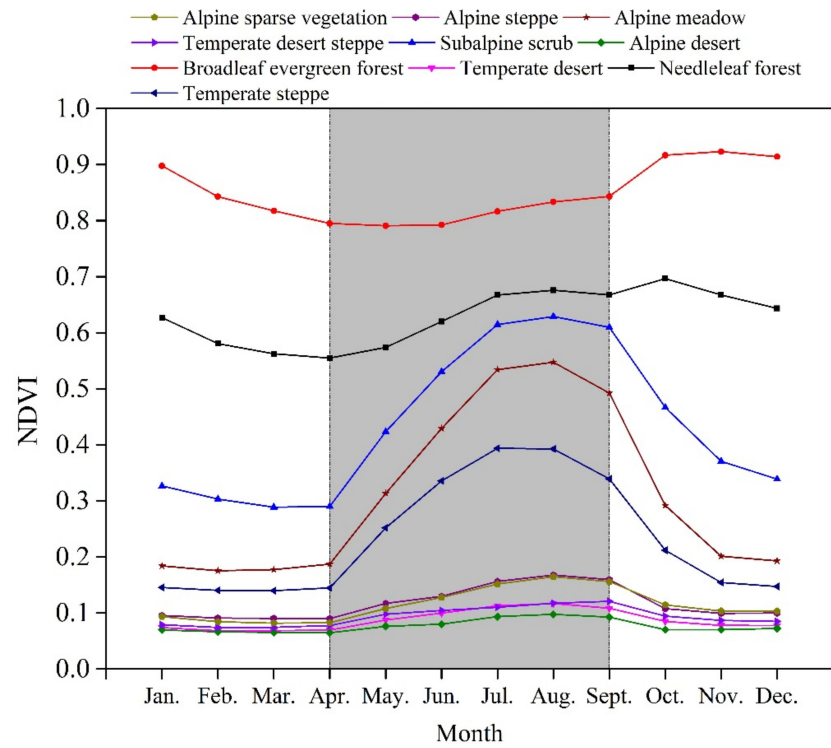


Figure 4. The annual variation of the monthly average NDVI for each vegetation type on the Tibetan Plateau from 1985 to 2015. The period from April to September is the analysis period in each year.

Mann–Kendall and Sen’s slope estimator were used to analyze the NDVI variation trends of vegetation on the Tibetan Plateau. The change trend was divided into five levels: significant increase, slight increase, remaining stable, slight decrease and significant decrease. A significant increase or decrease indicates that the change trend passes the significance level test at 0.01, and a slight increase or decrease indicates that the change trend passes the significance level test at 0.05. The change trend proportion of each type of vegetation is shown in Figure 5. The bars indicate the proportion of the area that demonstrated each change trend.

The change trends show significant differences among the different types of vegetation. The change trends of vegetation were dominated by increasing trends in alpine steppe, alpine desert, temperate desert steppe, alpine sparse vegetation, temperate desert and temperate steppe. These vegetation types are mainly distributed in the northwest area of the Tibetan Plateau. Among them, the increasing trend for NDVI in the alpine desert was the most obvious. The change trends for vegetation were also dominated by decreasing trends in alpine meadow, subalpine scrub, needleleaf forest, and broadleaf evergreen forest. These types of vegetation are mainly distributed in the southeastern area of the Tibetan Plateau, which is a relatively low-altitude area with sufficient water and hot climate conditions, and their NDVI values are at a higher level than in other regions (Figure 6). The NDVI of the broadleaf evergreen forest, which is distributed on the edge of the southeastern region of the Tibetan Plateau (93° E, 28° N), shows a more obvious decreasing trend than other vegetation types in recent years.

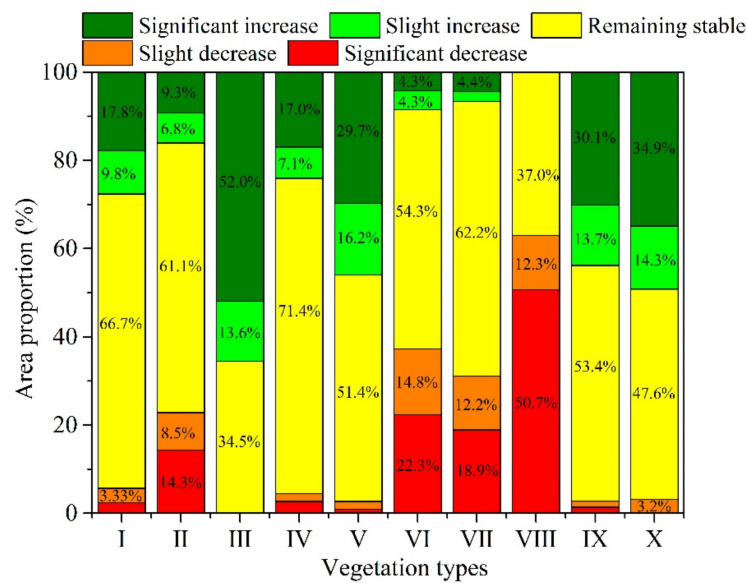


Figure 5. The proportion of the area that demonstrated each change trend on the Tibetan Plateau from 1985 to 2015. A significant increase or decrease indicates that the data passed the significance level test at 0.01. A slight increase or decrease indicates that the data passed the significance level test at 0.05. (I) Alpine steppe, (II) Alpine meadow, (III) Alpine desert, (IV) Temperate desert steppe, (V) Alpine sparse vegetation, (VI) Subalpine scrub, (VII) Needleleaf forest, (VIII) Broadleaf evergreen forest, (IX) Temperate desert, (X) Temperate steppe.

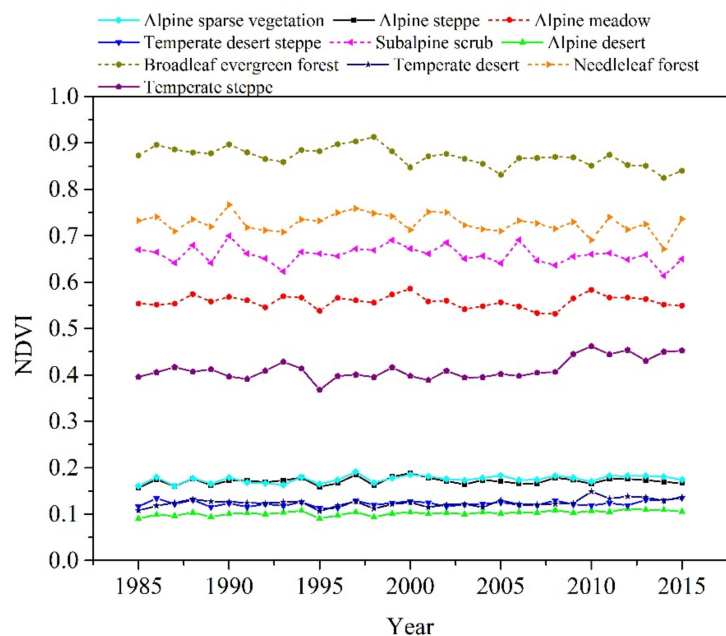


Figure 6. The average NDVI trend during the growing season for all types of vegetation from 1985 to 2015. The dashed line indicates that the NDVI of this vegetation type showed a decreasing trend during the study period. The solid line indicates that the NDVI of this vegetation type showed an increasing trend.

Based on previous knowledge, we took the alpine desert and broadleaf evergreen forest as examples of changing vegetation. We analyzed the relationship between the average monthly NDVI of each year for the two types of vegetation and the climate in recent years. The NDVI variation in the alpine desert showed a significant increasing trend,

while that of the broadleaf evergreen forest showed a significant decreasing trend. We also compared these two types of vegetation with the alpine meadow, where the overall regional level of NDVI change trend presented a state of equilibrium.

As shown in Figure 7, there are significant differences in the variation trends of climate factors in different regions, and there are significant differences in the influence on vegetation due to the comprehensive effects of climate factors. The temperature increased significantly in all three vegetation types ($p < 0.01$, indicating that the slope is significantly different from zero at 0.01 level) except for the minimum temperature in broadleaf evergreen forest. The average temperature change rates in the alpine desert, alpine meadow, and broadleaf evergreen forest regions were $0.059\text{ }^{\circ}\text{C year}^{-1}$, $0.048\text{ }^{\circ}\text{C year}^{-1}$ and $0.021\text{ }^{\circ}\text{C year}^{-1}$, respectively. There have also been differences in local temperature changes, and the warming rate of the broadleaf evergreen forest area is lower than that of other regions. This also indicates that the sensitivity to temperature change in different regions is different, and the temperature increase rate in the low-temperature region is faster than that in the high-temperature region. This finding can also be obtained from the change rates of the average minimum or maximum temperature: the change rates of the average maximum temperature of the three groups are $0.034\text{ }^{\circ}\text{C year}^{-1}$, $0.0405\text{ }^{\circ}\text{C year}^{-1}$, and $0.055\text{ }^{\circ}\text{C year}^{-1}$, and the change rates of the average minimum temperature of the three groups are $0.093\text{ }^{\circ}\text{C year}^{-1}$, $0.073\text{ }^{\circ}\text{C year}^{-1}$, and $0.018\text{ }^{\circ}\text{C year}^{-1}$, respectively. We can see that the average minimum temperature in the cold region is changing at a very fast rate.

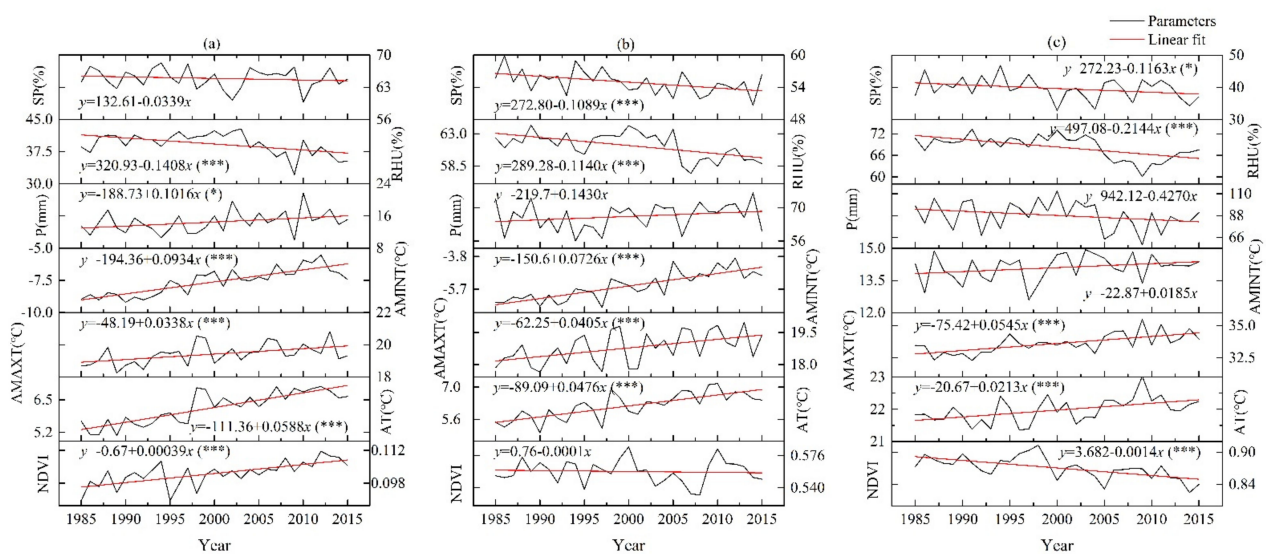


Figure 7. The trends in NDVI during the growing season for the three types of vegetation (a): alpine desert; (b): alpine meadow; (c): broadleaf evergreen forest) and the corresponding regional climate factors from 1985 to 2015. The average temperature, average maximum temperature, average minimum temperature, precipitation, relative humidity, and sunshine percentage are denoted as AT, AMAXT, AMINT, P, RHU, and SP, respectively. The *, **, *** indicate the slope is significantly different from zero (no trend) at the 0.1, 0.05, 0.01 level, respectively.

In addition to temperature, climate factors such as precipitation, relative humidity, and monthly sunshine percentage also presented evident change trends. The relative humidity showed a significant decline ($p < 0.01$) in all three vegetation types during the study period. The sunshine percentage also showed a declining trend in the three vegetation types, among which the sunshine percentage declined the most significantly in the alpine meadow ($p < 0.01$), followed by broadleaf evergreen forest ($p < 0.1$). The variation trend in the monthly sunshine percentage is $-0.0339\% \text{ year}^{-1}$, $-0.1089\% \text{ year}^{-1}$, and $-0.1163\% \text{ year}^{-1}$ in the alpine desert, alpine meadow, and broadleaf evergreen forest, respectively. This finding indicates that the sunshine percentage during the growing season

on the Tibetan Plateau has decreased in recent years. However, in the broadleaf evergreen forest zone, the decrease in sunshine percentage did not correspond to an increase in precipitation. The relative humidity of this region showed a significant decreasing trend (-0.2144% year $^{-1}$), indicating that the climate is becoming drier. The precipitation change trends were ecosystem-specific. The precipitation change rates in the three regions are 0.102 mm year $^{-1}$ ($p < 0.1$), 0.143 mm year $^{-1}$, and -0.427 mm year $^{-1}$, respectively. The precipitation in the alpine desert region and the alpine meadow region shows an increasing change trend. In contrast, the change in precipitation in the broadleaf evergreen forest region shows a significant decreasing trend.

The variation trends in NDVI for the three types of vegetation are 0.000387 year $^{-1}$, -0.0001 year $^{-1}$ and -0.001406 year $^{-1}$, respectively. The trend of NDVI of the alpine desert significantly increased ($p < 0.01$). The NDVI of the alpine meadow showed a slightly declining trend. The NDVI of the broadleaf evergreen forest showed a significantly declining trend ($p < 0.01$). Although the regional air temperature increased significantly, the percentage of monthly sunshine in the alpine meadow region showed a more significant decreasing trend. Because the influence of climate factors on NDVI is the result of the combined action of several factors, the main factor limiting vegetation growth in this region may be the decrease of sunshine.

As shown in Figure 6, four kinds of vegetation showed high NDVI values on the Tibetan Plateau, namely, in order of NDVI value: broadleaf evergreen forest, needleleaf forest, subalpine scrub, and alpine meadow. Their vegetation activities all showed a decreasing trend, and the decrease rates were, in order, broadleaf evergreen forest, needleleaf forest, subalpine scrub, and alpine meadow. The higher the NDVI value of the vegetation, the faster the rate of NDVI reduction, which indicates that the reduction of sunlight affects the growth of these vegetation types, to some extent. The other vegetation types with lower NDVI values showed increasing trends in each year. Compared with sunshine duration, temperature becomes the dominant parameter for vegetation growth on these vegetation types, and significantly increased temperature may be more related to the increased NDVI of these vegetation types.

3.2. Correlation Analysis between the NDVI in Different Vegetation Types and Climatic Factors

The lag effect of the response of vegetation growth to climate has been demonstrated in many studies. According to the results of this study, the response of vegetation to various climatic factors is significantly different in different vegetation types and growth stages.

On the whole, the response of NDVIs to temperature is more significant than that to other factors, and the lag period varies greatly due to the different growth stages and vegetation types, namely, alpine meadow, alpine desert, temperate desert steppe, alpine sparse vegetation and temperate desert. The hysteresis correlation coefficient indicates that the lag in the response of NDVIs to the average temperature and average maximum temperature is not obvious, while the lag in the response of NDVIs to the average minimum temperature is 1 or 2 months (Figure 8).

The NDVI of the alpine steppe, alpine desert, temperate desert steppe, alpine sparse vegetation, temperate desert and temperate steppe shows a more significant response to precipitation than to other climate factors. Desert vegetation is the most sensitive to precipitation, followed by grassland vegetation, and finally shrub and tree vegetation. For most types of vegetation, there is little correlation between NDVIs and precipitation at the start of the growing season. The correlation between NDVIs and precipitation tends to show a single peak during the growing season. This correlation increases gradually and reaches a peak in July or August and then decreases gradually, which is related to the change in the water utilization rate of vegetation. In particular, the correlation between the NDVI of the temperate desert and precipitation gradually increased during the whole growing season. Therefore, precipitation may be the main factor affecting the end of the growing season, and it is also the limiting parameter for the whole growing season of this vegetation type. In terms of lag, the influence of precipitation on NDVIs generally

occurs with a lag period of 1 or 2 months. The correlation coefficients showed that the precipitation in May and June had the greatest impact on the NDVI of the alpine steppe, alpine sparse vegetation, and temperate desert vegetation types, and the precipitation in June and July had a greater impact on the NDVI of the alpine desert, temperate desert and temperate steppe.

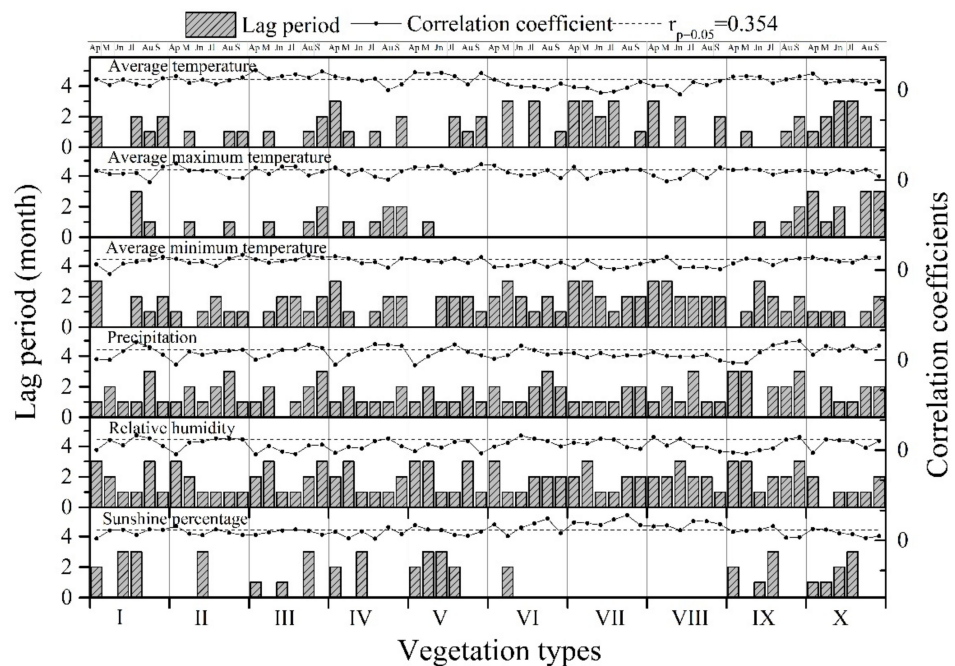


Figure 8. Correlation coefficient and lag time for each vegetation type during the growing season (i.e., from April to September). The dash lines are at the statistical significance of 0.05. (I) Alpine steppe, (II) Alpine meadow, (III) Alpine desert, (IV) Temperate desert steppe, (V) Alpine sparse vegetation, (VI) Subalpine scrub, (VII) Needleleaf forest, (VIII) Broadleaf evergreen forest, (IX) Temperate desert, (X) Temperate steppe.

The subalpine scrub, needle leaf forest and broadleaf evergreen forest were most sensitive to sunshine percentage with a lag period of 0 months, indicating that the vegetation response to sunshine within 1 month. Compared with temperature and precipitation, the effect of sunlight on vegetation growth for these vegetation types was more significant.

Figure 9 shows the spatial distribution of the lag effects of NDVIs to average temperature, precipitation, relative humidity and sunshine percentage. The response of NDVIs to average temperature exhibits 1, 2, 3 months lag in February, May and June, respectively, in the western region of the Tibetan Plateau, indicating that the temperature in March can highly affect the vegetation growth at the early stage of the growing season. In August and September, the vegetation is mainly affected by the average temperature of July. The result shows that the precipitation had the greatest influence on vegetation growth in May and June in the western regions of the Tibetan Plateau, which mainly distribute temperate desert steppe and alpine steppe. The relative humidity affects vegetation growth in September with a 0-month lag period in most regions of the Tibetan Plateau; that is, the relative humidity in September had significant effects on vegetation.

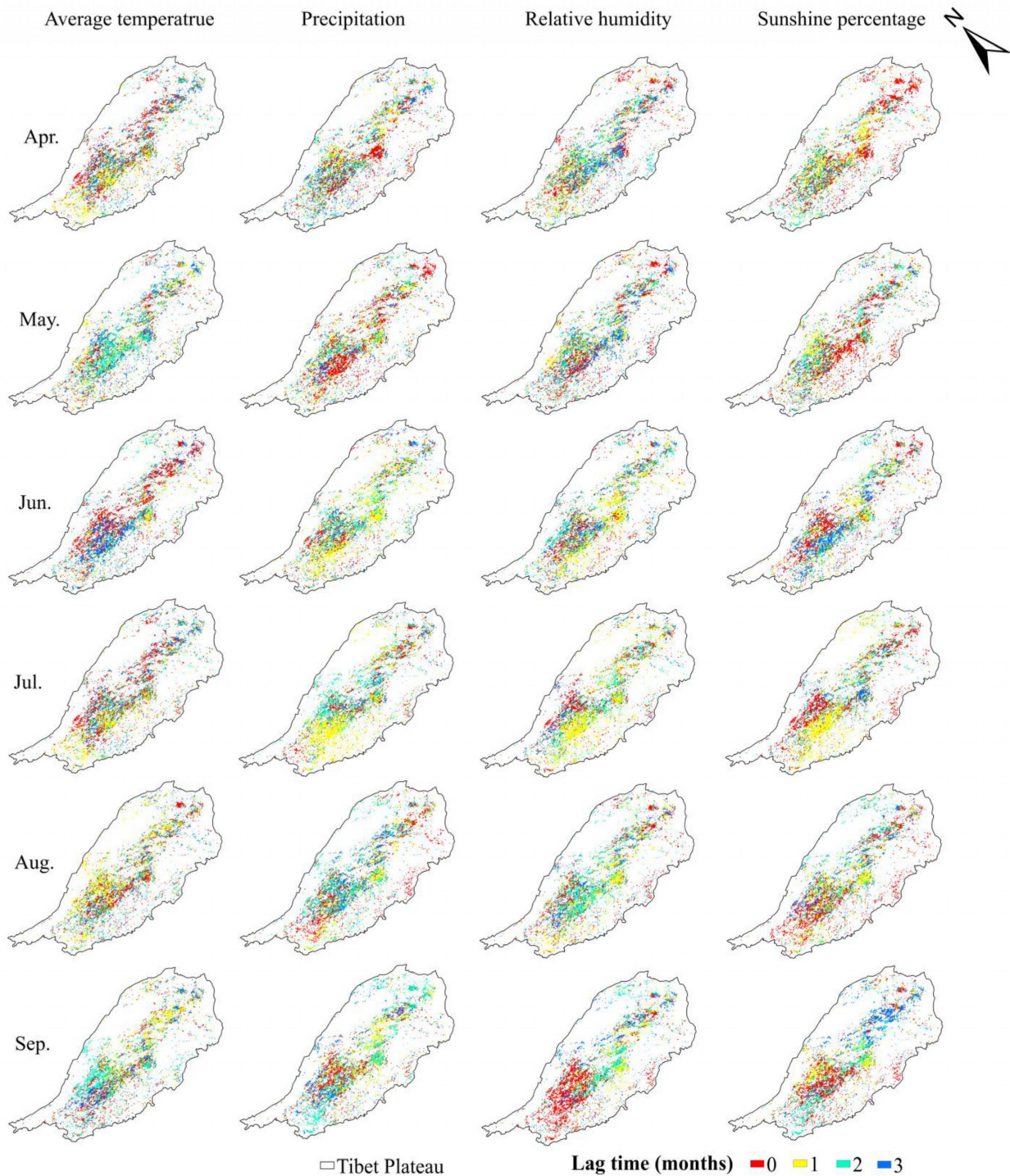


Figure 9. Spatial distribution of the response lag time of the NDVI to average temperature, precipitation, relative humidity and sunshine percentage in different growth stages (from April to September) over the Tibetan Plateau.

In April, sunshine percentage had a direct influence on the vegetation in the eastern part of the Tibetan Plateau. However, there were different degrees of lag response of NDVIs to sunshine in the western regions of the Tibetan Plateau.

3.3. Interpretation of NDVI Variation with Climatic Factors

The stepwise regression was adopted to calculate the main factors affecting the NDVIs with the consideration of lag effects. The results were shown in Figure 10. The sunshine per-

centage greatly influences the needleleaf forest, broadleaf evergreen forest, and subalpine scrub during the growing season. Previous studies have shown that approximately 13–19% of global regions have experienced changes in growing season length, and approximately 30% of the changes occurred in the northern alpine biome in the northern hemisphere [29]. Therefore, it is of significance to study the main climatic factors that affect vegetation at the start and end of growing season: The initial growth period (i.e., in April) for the needleleaf forest, broadleaf evergreen forest, and subalpine scrub is greatly influenced by the sunshine percentage, where the three vegetation types are located in the southeastern Tibetan Plateau with a lower altitude than the western region. These three vegetation types are also affected by sunshine percentage during the whole growing season. The alpine steppe located in the western Tibetan Plateau is greatly affected by sunshine percentage in April and September. The temperate desert, temperate steppe, alpine desert, temperate desert steppe, and alpine meadow were mainly affected by air temperature in April. In September, we can see the temperate desert, temperate steppe, and temperate desert steppe are precipitation-dominated vegetation; alpine steppe, alpine desert, alpine meadow, and alpine sparse vegetation are temperature-dominated vegetation.

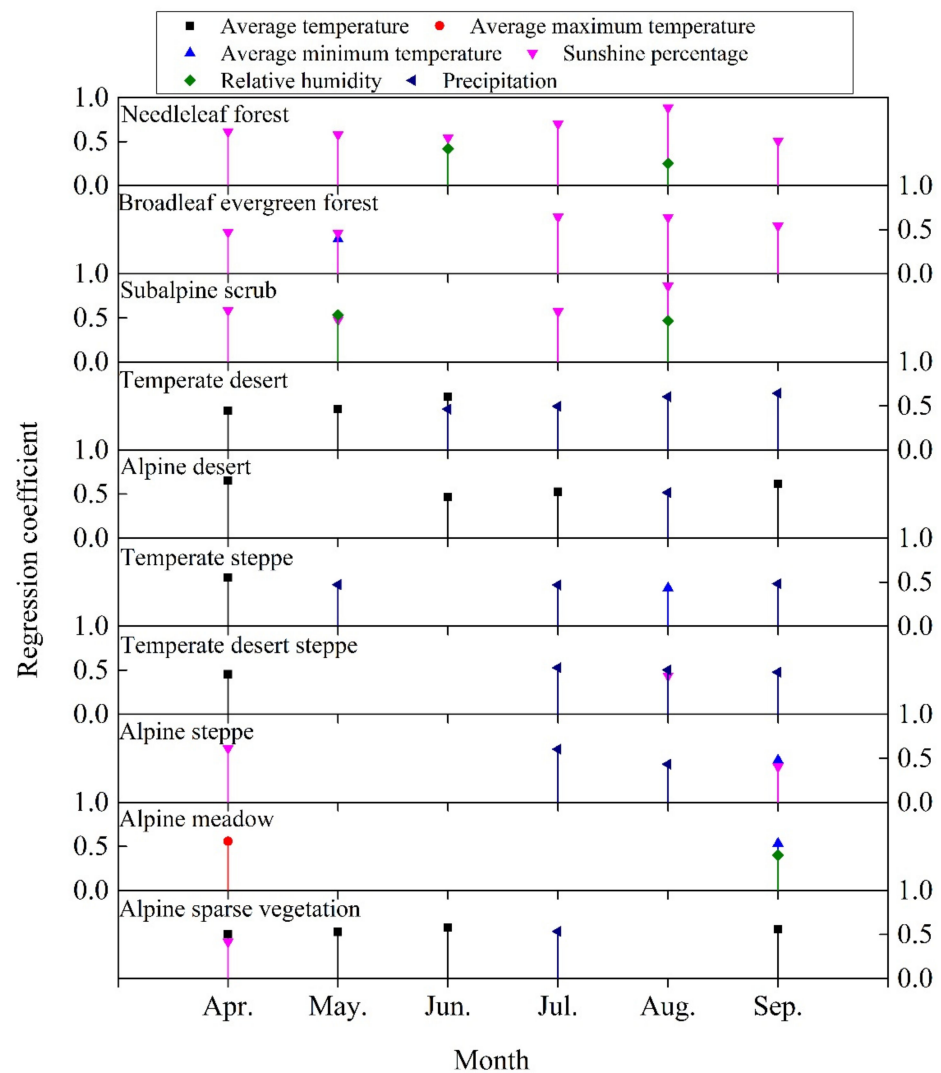


Figure 10. Selected climatic variables and regression coefficients of these variables to the NDVI of each vegetation type in each month during the growing season (April to September). Note that there is no significant influencing variable in some growing stages of some vegetation types.

4. Discussion

4.1. Change Trends of Climate Factors and NDVI on the Tibetan Plateau

Based on the GIMMS NDVI3g data, the NDVI variation trend on the Tibetan Plateau in the last 31 years presents strong heterogeneity in different vegetation ecosystems (Figure 5), but increases dominate the overall change trend. Generally, vegetation types (subalpine scrub, needleleaf forest and broadleaf evergreen forest) with a large proportion of decreasing NDVIs were distributed in the southeastern region of the Tibetan Plateau (Figures 3 and 5). In particular, a large area (about 23% of total pixels) of NDVI decline also exists in alpine meadow. Due to drastic changes in the environment, large areas of grassland degradation had appeared on the Tibetan Plateau before the 1980s, and the alpine grassland and alpine marsh meadow vegetation in the Maduo and Tuotuo river areas had been degraded on a large scale. A study has shown that the enhanced precipitation reduced the microbial diversity in alpine grassland soils, and the alpine steppe could be more resistant to environmental changes than the alpine meadow [30]. Considering that the NDVI in degraded grasslands will not be significantly increased with the improvement of climate conditions over a short period, this may also be the main reason that the NDVI of alpine grassland did not increase significantly, especially in alpine meadow. The GIMMS3g data underestimated the greening trend on the Tibetan Plateau [31] mainly because of the impacts of sensor shifts and degradation, especially at the break point of sensor shifts [32,33]. According to the research results of [13], the GIMMS NDVI data from 2000 to 2006 showed an inconsistent trend with the SPOT-VGT data and MODIS data from the same period, showing a significant decrease in NDVIs, especially on the western Tibetan Plateau. Therefore, the overall NDVI-increase area on the Tibetan Plateau may be larger than that indicated by this paper.

The increased temperature and decreased sunshine percentage dominate the whole region of the Tibetan Plateau during the study period. As shown in Figure 7, the percentage of monthly sunshine on the Tibetan Plateau is decreasing in all three vegetation types. You et al. (2010) also found that the mean annual sunshine duration showed a significant decrease from 1983 to 2005 [34]. Generally, sunshine duration is mainly influenced by cloud cover or aerosols, and an increase in cloud cover or in the aerosol concentration emitted by humans results in a decrease in the sunshine duration [35]. Moreover, some studies also show that the monsoon intensification of the Indian summer monsoon may result in increasing cloud coverage in the southeastern Tibetan Plateau, reducing the sunshine duration [16,36]. Of the entire degraded grassland, 56.74% has been proven to be due to climate change from 2001 to 2013 on the Tibetan Plateau, with radiation being more related to climate-induced grassland degradation than other climate parameters [37]. The results in this paper also show that the vegetation types with a decreasing NDVI in the southeastern Tibetan Plateau are greatly affected by sunshine percentage (the needleleaf forest, broadleaf evergreen forest, and subalpine scrub in Figure 10). Most vegetation types in the western regions have seen an increasing NDVI, where these regions have seen more rapid warming than the southeastern Tibetan Plateau.

4.2. Lag in the NDVI Response to Precipitation and Temperature

Studies have confirmed that the influence of precipitation on vegetation shows a certain hysteresis. Precipitation is first converted to soil water before it can be absorbed by plants for transpiration, which is the driving force behind water and nutrient uptake by vegetation. The process by which precipitation is converted into water available for vegetation is related to the soil type, land cover, physiological characteristics of the vegetation, climate conditions and so on [38]. Due to the different soil types and topography, the soil water holding capacity is different in different areas. Some soils can retain water for a long time after rainfall, which has a lasting impact on vegetation growth. In addition, deep-rooted plants may have a longer “memory” for precipitation [22,39]. Many woody plant species utilized only cold season rain for growth [40]. The results (Figure 8) also showed no significant relationship between the NDVI of the needleleaf forest, subalpine

scrub, and broadleaf evergreen forest and precipitation during the growing season. The correlation coefficients between NDVIs of the needleleaf forest, broadleaf evergreen forest, and precipitation reached the peak in April.

As shown in Figure 9, the temperature in March greatly influenced vegetation growth at the initial stage of growing season over western regions of the Tibetan Plateau. The lag effects were evident in these regions. Some possible arguments are that the temperature can affect soil microbial activities, then have lasting effects on vegetation growth [41]; additionally, temperature affects the melting of glaciers and permafrost at high altitudes, increasing runoff in some river systems [37,42].

4.3. Possible Mechanisms of Climate Influences on Vegetation

Precipitation rarely affects NDVIs at the start of growing season, as shown in Figure 10 in April. According to the research of Yang and Piao (2006), in the low-temperature environment of the Tibetan Plateau at the beginning of growing season, precipitation can promote the growth of vegetation only after microorganisms regulate the N and P cycles [41]. The activity of microorganisms is highly correlated with both the air temperature and soil temperature, which are related to radiation. This conclusion is a good explanation for why the rainfall and NDVIs in the early stage of growing season are hardly correlated.

Sunshine can affect vegetation in a variety of ways. Sunlight is also a major factor causing vegetation degradation on the Tibetan Plateau, contributing to large areas of climate-induced vegetation degradation [37]. According to Graham et al. (2003), the changes in solar radiation caused by clouds and aerosols mainly affect the growth of plants by affecting the absorption of carbon dioxide by vegetation [35]. Moreover, radiation can affect turbulent surface energy flux, part of which provides the driving force for evapotranspiration [43]. In this way, radiation can affect vegetation transpiration in coordination with soil moisture in real time. In the needleleaf forest, subalpine scrub, and broadleaf evergreen forest ecosystems, which are heat- and water-abundant regions, vegetation is greatly affected by sunshine duration, as shown in Figure 10. These vegetation types mainly distributed in the southeastern Tibetan Plateau, which is consistent with the result of the previous study [16,44], and one argument for the high sensitivity of the needleleaf forest and shrub to sunshine may be that the southeastern Tibetan Plateau receives less solar energy and shorter sunshine duration than other areas [16]. Decreasing precipitation and sunshine percentage and increasing temperature in these regions interactively make it drier than before [16], affecting vegetation growth. At the same time, the warming rate in the southwestern part is slower than in western regions, as shown in the comparison of the three vegetation types in Figure 7. Therefore, the temperature may play a limited role in NDVI variation in the southwestern region. Conversely, the significantly increasing trend makes temperature the main factor affecting the NDVI of most vegetation types in the western and northeastern Tibetan Plateau. It is worth noting that the alpine steppe is also sensitive to sunshine percentage in April, as shown in Figure 10. The sunshine percentage may affect the growth of the alpine steppe in the early growing season in the following ways: sunlight can provide energy to soil and raise soil temperature, promoting the regulation of N and P cycles in the soil [41]. Moreover, warming soil causes snowmelt and affects glaciers melting process in high-elevation regions, providing more water for the alpine steppe [16,45].

Precipitation is not a significant parameter for the alpine meadow during the whole growing season. We can see from Figure 7b, the average monthly precipitation in the alpine meadow region was 60–80 mm. One possible argument is that vegetation would not be affected by precipitation when the precipitation exceeds a certain threshold [20,21], which is abundant for the alpine meadow. The alpine meadow has seen significantly decreasing relative humidity and sunshine percentage, as shown in Figure 7b. Simultaneously, the relative humidity and average minimum temperature have significant positive effects on alpine meadow vegetation in September, according to the regression results shown in Figure 10. The alpine meadow is widely distributed in the Tibetan Plateau, mainly in the

central and eastern regions. Some regions receive shorter sunshine duration than other parts of the Tibetan Plateau. Relative humidity can affect the transpiration of vegetation and nutrient migration by influencing the atmospheric water potential. Moreover, lower humidity can cause stomatal closure, which prevents carbon dioxide from being absorbed by the vegetation, reducing photosynthesis activities, thus affecting NDVIs. Therefore, for alpine meadows, sunshine percentage and humidity may be the principal climatic factors affecting this type of vegetation. The reduction in humidity and sunshine percentage caused a slight decrease in the NDVI of alpine vegetation even though the temperature increased significantly.

Although some uncertainty exists in vegetation type change due to the limitations in the dataset (there is only one period of vegetation type dataset) during such an extended study period, pure pixels can reduce the probability of the shift of dominant vegetation type to some extent because there is only a single vegetation type in these pixels. Therefore, the regression results can reflect the effects of climate factors on each vegetation ecosystem. However, there are also some limitations in this study. The interpolation results of climate parameters may have larger errors in the western region (mainly including the alpine steppe, alpine desert, temperate desert steppe, and temperate desert) of the Tibetan Plateau with sparse meteorological stations than in eastern parts. Therefore, more auxiliary data need to be introduced to improve the interpolation accuracy of meteorological parameters in further study. One feasible idea is to find a more suitable covariable for climate parameters interpolation. Moreover, sun-sensor geometry, such as Solar-to-sensor angle, can significantly affect NDVIs, mainly due to the visibility of shadows [46–48], especially in winter in evergreen conifer systems and dryland vegetation systems. Therefore, annual NDVI variation may be partly induced by sun-sensor geometry in the broadleaf evergreen forest, needleleaf forest, temperate desert and alpine desert. Correcting remote sensing data for sun-sensor geometry effects is important to isolate the response of vegetation to climate factors, which is a target for further research.

5. Conclusions

The interannual NDVI for the Tibetan Plateau shows an overall increasing trend, but there is strong spatial heterogeneity. The NDVI of the alpine desert increased the most significantly of all studied vegetation types. The NDVI values of four types of vegetation, namely, alpine meadow, subalpine scrub, needleleaf forest and broadleaf evergreen forest, showed a decreasing trend, and their NDVI values were typically larger than those of the other vegetation types.

The responses of vegetation to temperature, precipitation and relative humidity have certain lag periods. The alpine meadow, alpine desert, temperate desert steppe and temperate desert respond more significantly to temperature than to other climate factors, and the length of the lag period varies greatly in different vegetation ecosystems and growth stages. The desert vegetation is the most sensitive to precipitation, followed by grassland vegetation and finally shrubs. The response of NDVIs to precipitation generally occurs with a lag period of 1 or 2 months. During the whole growing season, the correlation between NDVIs and precipitation first increased to reach a peak and then decreased.

At the start of the growing season, temperature is the main climatic factor that affects the NDVI of most vegetation types. After that, precipitation begins to have an effect on vegetation. The sunshine duration has a relatively significant impact on the NDVI of the subalpine scrub, needleleaf forest, and broadleaf evergreen forest with a short lag period (within one month) during almost the whole growing season. At the end of the growing season, the temperate desert, temperate steppe, and temperate desert steppe are greatly affected by precipitation; alpine steppe, alpine desert, alpine meadow, and alpine sparse vegetation are greatly affected by temperature, especially for alpine steppe and alpine meadow affected by monthly minimum temperature.

This study mainly provided an overview of how different climate parameters affect different domain types of vegetation on the Tibetan Plateau. These findings will provide a better

understanding of the climate change trends and contribute to the general knowledge of the drivers and mechanisms of ecosystem-dependent vegetation degradation on the Tibetan Plateau. For further study, high spatial and temporal resolution data are required for more accurate analyses of the lag effects and ecological mechanisms.

Author Contributions: Shuohao Cai conceived and designed this study, carried out the analysis and drafted the manuscript. Xiaoning Song administrated the study, gave some constructive suggestions and applied for funding for this study. Ronghai Hu participated in the design of the study and revised the draft to improve the presentation of this study. Da Guo offered some suggestions on visualization and the draft. All authors have read and agreed to the published version of the manuscript.

Funding: This research has been funded by grants from National Natural Science Foundation of China, No. 42041005 and the National Key Research and Development Program of China, No. 2016YFC0501800/2016YFC0501801.

Data Availability Statement: The data that support the findings of this study are available from the third party mentioned above in this article. Restrictions apply to the availability of these data, which were used under license for this study. Data are available with the permission of them (URLs are listed in the article corresponding with the institutions).

Acknowledgments: The authors are very grateful for the China Meteorological Data Service Centre (<http://data.cma.cn/> accessed on 14 April 2021) for providing climate data and the Ecological Forecasting Lab at NASA Ames Research Centre (<https://ecocast.arc.nasa.gov/> accessed on 14 April 2021) for providing NDVI data, and the Resource and Environment Data Cloud Platform for providing vegetation data.

Conflicts of Interest: No potential conflict of interest was reported by the authors.

References

1. Cui, X.; Graf, H.-F. Recent land cover changes on the Tibetan Plateau: A review. *Clim. Chang.* **2009**, *94*, 47–61. [[CrossRef](#)]
2. Piao, S.; Fang, J.; Ji, W.; Guo, Q.; Ke, J.; Tao, S. Variation in a satellite-based vegetation index in relation to climate in China. *J. Veg. Sci.* **2004**, *15*, 219–226. [[CrossRef](#)]
3. Pang, G.; Wang, X.; Yang, M. Using the NDVI to identify variations in, and responses of, vegetation to climate change on the Tibetan Plateau from 1982 to 2012. *Quat. Int.* **2017**, *444*, 87–96. [[CrossRef](#)]
4. Potter, C.S.; Brooks, V. Global analysis of empirical relations between annual climate and seasonality of NDVI. *Int. J. Remote Sens.* **1998**, *19*, 2921–2948. [[CrossRef](#)]
5. Tucker, C.J. Red and photographic infrared linear combinations for monitoring vegetation. *Remote Sens. Environ.* **1979**, *8*, 127–150. [[CrossRef](#)]
6. Tucker, C.J.; Sellers, P.J. Satellite remote sensing of primary production. *Int. J. Remote Sens.* **1986**, *7*, 1395–1416. [[CrossRef](#)]
7. Pettorelli, N.; Vik, J.O.; Mysterud, A.; Gaillard, J.-M.; Tucker, C.J.; Stenseth, N.C. Using the satellite-derived NDVI to assess ecological responses to environmental change. *Trends Ecol. Evol.* **2005**, *20*, 503–510. [[CrossRef](#)]
8. Guo, B.; Zhou, Y.; Wang, S.-X.; Tao, H.-P. The relationship between Normalized Difference Vegetation Index (NDVI) and climate factors in the semiarid region: A case study in Yalu Tsangpo River basin of Qinghai-Tibet Plateau. *J. Mt. Sci.* **2014**, *11*, 926–940. [[CrossRef](#)]
9. Ma, M.G.; Veroustraete, F. Interannual change trend of NDVI from 1981 to 2001 in the Heihe River Basin, China. In *Proceedings of the 2nd International Vegetation User Conference, Antwerp, Belgium, 24–26 March 2004*; European Commission: Bruxelles, Belgium, 2004; pp. 231–237.
10. Prasad, V.K.; Badarinath, K.V.S.; Eaturu, A. Effects of precipitation, temperature and topographic parameters on evergreen vegetation greenery in the Western Ghats, India. *Int. J. Clim.* **2008**, *28*, 1807–1819. [[CrossRef](#)]
11. Farrar, T.; Nicholson, S.; Lare, A. The influence of soil type on the relationships between NDVI, rainfall, and soil moisture in semiarid Botswana. II. NDVI response to soil moisture. *Remote Sens. Environ.* **1994**, *50*, 121–133. [[CrossRef](#)]
12. White, M.A.; Thornton, P.; Running, S.W. A continental phenology model for monitoring vegetation responses to interannual climatic variability. *Glob. Biogeochem. Cycles* **1997**, *11*, 217–234. [[CrossRef](#)]
13. Li, L.; Zhang, Y.; Liu, L.; Wu, J.; Li, S.; Zhang, H.; Zhang, B.; Ding, M.; Wang, Z.; Paudel, B. Current challenges in distinguishing climatic and anthropogenic contributions to alpine grassland variation on the Tibetan Plateau. *Ecol. Evol.* **2018**, *8*, 5949–5963. [[CrossRef](#)]
14. Woodward, F.I.; Lomas, M.R.; Kelly, C.K. Global climate and the distribution of plant biomes. *Philos. Trans. R. Soc. B Biol. Sci.* **2004**, *359*, 1465–1476. [[CrossRef](#)] [[PubMed](#)]
15. Zhang, X.; Wu, S.; Yan, X.; Chen, Z. A global classification of vegetation based on NDVI, rainfall and temperature. *Int. J. Clim.* **2016**, *37*, 2318–2324. [[CrossRef](#)]

16. Wang, H.; Liu, D.; Lin, H.; Montenegro, A.; Zhu, X. NDVI and vegetation phenology dynamics under the influence of sunshine duration on the Tibetan plateau. *Int. J. Clim.* **2014**, *35*, 687–698. [[CrossRef](#)]
17. Lin, S.; Moore, N.J.; Messina, J.P.; Wu, J. Evaluation of MODIS surrogates for meteorological humidity data in East Africa. *Int. J. Remote Sens.* **2013**, *34*, 4669–4679. [[CrossRef](#)] [[PubMed](#)]
18. Woodward, F.; McKee, I. Vegetation and climate. *Environ. Int.* **1991**, *17*, 535–546. [[CrossRef](#)]
19. Capecchi, V.; Crisci, A.; Lorenzo, G.; Maselli, F.; Vignaroli, P. Analysis of NDVI trends and their climatic origin in the Sahel 1986–2000. *Geocarto Int.* **2008**, *23*, 297–310. [[CrossRef](#)]
20. Davenport, M.L.; Nicholson, S.E. On the relation between rainfall and the Normalized Difference Vegetation Index for diverse vegetation types in East Africa. *Int. J. Remote Sens.* **1993**, *14*, 2369–2389. [[CrossRef](#)]
21. Martiny, N.; Camberlin, P.; Richard, Y.; Philippon, N. Compared regimes of NDVI and rainfall in semi-arid regions of Africa. *Int. J. Remote Sens.* **2006**, *27*, 5201–5223. [[CrossRef](#)]
22. Philippon, N.; Mougin, E.; Jarlan, L.; Frison, P.-L. Analysis of the linkages between rainfall and land surface conditions in the West African monsoon through CMAP, ERS-WSC, and NOAA-AVHRR data. *J. Geophys. Res. Space Phys.* **2005**, *110*, 110. [[CrossRef](#)]
23. Piao, S.; Fang, J.; Zhou, L.; Guo, Q.; Henderson, M.; Ji, W.; Li, Y.; Tao, S. Interannual variations of monthly and seasonal Normalized Difference Vegetation Index (NDVI) in China from 1982 to 1999. *J. Geophys. Res. Space Phys.* **2003**, *108*. [[CrossRef](#)]
24. Wen, Z.; Wu, S.; Chen, J.; Lü, M. NDVI indicated long-term interannual changes in vegetation activities and their responses to climatic and anthropogenic factors in the Three Gorges Reservoir Region, China. *Sci. Total Environ.* **2017**, *574*, 947–959. [[CrossRef](#)] [[PubMed](#)]
25. Holben, B.N. Characteristics of maximum-value composite images from temporal AVHRR data. *Int. J. Remote Sens.* **1986**, *7*, 1417–1434. [[CrossRef](#)]
26. Gocic, M.; Trajkovic, S. Analysis of changes in meteorological variables using Mann-Kendall and Sen’s slope estimator statistical tests in Serbia. *Glob. Planet. Chang.* **2013**, *100*, 172–182. [[CrossRef](#)]
27. Yue, S.; Pilon, P.; Cavadias, G. Power of the Mann–Kendall and Spearman’s rho tests for detecting monotonic trends in hydrological series. *J. Hydrol.* **2002**, *259*, 254–271. [[CrossRef](#)]
28. Yang, Y.; Xu, J.; Hong, Y.; Lv, G. The dynamic of vegetation coverage and its response to climate factors in Inner Mongolia, China. *Stoch. Environ. Res. Risk Assess.* **2011**, *26*, 357–373. [[CrossRef](#)]
29. Garonna, I.; De Jong, R.; Schaepman, M.E. Variability and evolution of global land surface phenology over the past three decades (1982–2012). *Glob. Chang. Biol.* **2016**, *22*, 1456–1468. [[CrossRef](#)]
30. Zhang, Y.; Dong, S.; Gao, Q.; Liu, S.; Zhou, H.; Ganjurjav, H.; Wang, X. Climate change and human activities altered the diversity and composition of soil microbial community in alpine grasslands of the Qinghai-Tibetan Plateau. *Sci. Total Environ.* **2016**, *562*, 353–363. [[CrossRef](#)]
31. Li, W.; Haiying, Y.U.; Qiang, Z.; Yunjia, X.U.; Junhu, D. Responses of aboveground biomass of alpine grasslands to climate changes on the Qinghai-Tibet Plateau. *J. Geogr. Sci.* **2018**, *28*, 1953–1964. [[CrossRef](#)]
32. Zhang, Y.L.; Song, C.H.; Band, L.E.; Sun, G.; Li, J.X. Reanalysis of global terrestrial vegetation trends from MODIS products: Browning or greening? *Remote Sens. Environ.* **2017**, *191*, 145–155. [[CrossRef](#)]
33. Detsch, F.; Otte, I.; Appelhans, T.; Nauss, T. A comparative study of cross-product NDVI dynamics in the Kilimanjaro region—A matter of sensor, degradation calibration, and significance. *Remote Sens.* **2016**, *8*, 159. [[CrossRef](#)]
34. You, Q.; Kang, S.; Flügel, W.-A.; Sanchez-Lorenzo, A.; Yan, Y.; Huang, J.; Martin-Vide, J. From brightening to dimming in sunshine duration over the eastern and central Tibetan Plateau (1961–2005). *Theor. Appl. Clim.* **2009**, *101*, 445–457. [[CrossRef](#)]
35. Graham, E.; Mulkey, S.S.; Kitajima, K.; Phillips, N.G.; Wright, S.J. Cloud cover limits net CO₂ uptake and growth of a rainforest tree during tropical rainy seasons. *Proc. Natl. Acad. Sci. USA* **2003**, *100*, 572–576. [[CrossRef](#)] [[PubMed](#)]
36. Lau, K.M.; Kim, M.K.; Kim, K.M. Asian summer monsoon anomalies induced by aerosol direct forcing: The role of the Tibetan Plateau. *Clim. Dyn.* **2006**, *26*, 855–864. [[CrossRef](#)]
37. Wang, Z.; Zhang, Y.; Yang, Y.; Zhou, W.; Gang, C.; Zhang, Y.; Li, J.; An, R.; Wang, K.; Odeh, I.; et al. Quantitative assess the driving forces on the grassland degradation in the Qinghai–Tibet Plateau, in China. *Ecol. Inform.* **2016**, *33*, 32–44. [[CrossRef](#)]
38. Schwinning, S.; Sala, O. Hierarchy of responses to resource pulses in arid and semi-arid ecosystems. *Oecologia* **2004**, *141*, 211–220. [[CrossRef](#)] [[PubMed](#)]
39. Schwinning, S.; Sala, O.; Loik, M.E.; Ehleringer, J.R. Thresholds, memory, and seasonality: Understanding pulse dynamics in arid/semi-arid ecosystems. *Oecologia* **2004**, *141*, 191–193. [[CrossRef](#)]
40. Snyder, K.A.; Donovan, L.A.; James, J.J.; Tiller, R.L.; Richards, J.H. Extensive summer water pulses do not necessarily lead to canopy growth of Great Basin and northern Mojave Desert shrubs. *Oecologia* **2004**, *141*, 325–334. [[CrossRef](#)]
41. Yuan-He, Y.; Shi-Long, P. Variations in grassland vegetation cover in relation to climatic factors on the Tibetan Plateau. *Chin. J. Plant Ecol.* **2006**, *30*, 1–8. [[CrossRef](#)]
42. Käab, A.; Chiarle, M.; Raup, B.; Schneider, C. Climate change impacts on mountain glaciers and permafrost. *Glob. Planet. Chang.* **2007**, *56*, 7–9. [[CrossRef](#)]
43. Carlson, T. An overview of the “Triangle Method” for estimating surface evapotranspiration and soil moisture from satellite imagery. *Sensors* **2007**, *7*, 1612–1629. [[CrossRef](#)]
44. Du, J.; Zhao, C.; Shu, J.; Jiaerheng, A.; Yuan, X.; Yin, J.; Fang, S.; He, P. Spatiotemporal changes of vegetation on the Tibetan Plateau and relationship to climatic variables during multiyear periods from 1982–2012. *Environ. Earth Sci.* **2016**, *75*, 1–18. [[CrossRef](#)]

-
45. Chen, H.; Zhu, Q.; Peng, C.; Wu, N.; Wang, Y.; Fang, X.; Gao, Y.; Zhu, D.; Yang, G.; Tian, J.; et al. The impacts of climate change and human activities on biogeochemical cycles on the Qinghai-Tibetan Plateau. *Glob. Chang. Biol.* **2013**, *19*, 2940–2955. [[CrossRef](#)] [[PubMed](#)]
 46. Norris, J.R.; Walker, J.J. Solar and sensor geometry, not vegetation response, drive satellite NDVI phenology in widespread ecosystems of the western United States. *Remote Sens. Environ.* **2020**, *249*, 112013. [[CrossRef](#)]
 47. Fensholt, R.; Sandholt, I.; Proud, S.R.; Stisen, S.; Rasmussen, M.O. Assessment of MODIS sun-sensor geometry variations effect on observed NDVI using MSG SEVIRI geostationary data. *Int. J. Remote Sens.* **2010**, *31*, 6163–6187. [[CrossRef](#)]
 48. Morton, D.C.; Nagol, J.; Carabajal, C.C.; Rosette, J.; Palace, M.; Cook, B.D.; Vermote, E.F.; Harding, D.J.; North, P.R.J. Amazon forests maintain consistent canopy structure and greenness during the dry season. *Nat. Cell Biol.* **2014**, *506*, 221–224. [[CrossRef](#)]